

(c) To a solution of II (0.2 mmol) in dichloromethane (15 mL) was added dropwise at room temperature $P(t\text{-Bu})_2\text{Ph}$ (0.4 mmol) in the same solvent (5 mL). The reaction mixture was stirred for ~1 h. The solvent was removed under reduced pressure to give a pale orange solid that was shown by ^{31}P NMR spectral measurement to be a mixture of *trans*- $\text{PtCl}_2[\text{P}(t\text{-Bu})_2\text{Ph}]_2$ and $\text{Pt}_2(\mu\text{-Cl})_2\text{Cl}_2[\text{P}(t\text{-Bu})_2\text{Ph}]_2$. The quantity of *trans*- $\text{PtCl}_2[\text{P}(t\text{-Bu})_2\text{Ph}]_2$ increased with increasing rate of addition of the phosphine.

(d) III and $P(t\text{-Bu})_2\text{Ph}$, in a 1:4 mole ratio, were stirred (~3 h) together in dichloromethane. Removal of the solvent in vacuo and crystallization of the residue from dichloromethane/methanol gave yellow crystals of *trans*- $\text{PdCl}_2[\text{P}(t\text{-Bu})_2\text{Ph}]_2$; >90% yield: mp 221–225 °C dec; IR $\nu(\text{Pd-Cl})$ 350 cm^{-1} [lit.¹⁰ mp 222–226 °C dec; $\nu(\text{Pd-Cl})$ 350 cm^{-1}]; $^{31}\text{P}\{^1\text{H}\}$ NMR (CH_2Cl_2) δ 52.9. Anal. Calcd for $\text{C}_{28}\text{H}_{46}\text{P}_2\text{Cl}_2\text{Pd}$: C, 54.1; H, 7.5. Found: C, 53.88; H, 7.6.

(e) $P(t\text{-Bu})_2\text{Ph}$ (0.4 mmol) in THF (5 mL) was slowly added to a solution of III (0.2 mmol) in THF (10 mL). Removal of the solvent and repeated recrystallization of the resulting solid from dichloromethane/methanol gave dark red needles of $\text{Pd}_2(\mu\text{-Cl})_2\text{Cl}_2[\text{P}(t\text{-Bu})_2\text{Ph}]_2$ in ~70% yield: mp 220–224 °C dec; IR $\nu(\text{Pd-Cl})$ 355 vs, 307 m, 250 vs cm^{-1} [lit.¹⁰ mp 220–225 °C dec, $\nu(\text{Pd-Cl})$ 356 vs, 307 m, 250 vs cm^{-1}]; $^{31}\text{P}\{^1\text{H}\}$ NMR (CH_2Cl_2) δ 74.4 (s). Anal. Calcd for $\text{C}_{28}\text{H}_{46}\text{P}_2\text{Cl}_4\text{Pd}_2$: C, 42.1; H, 5.8; Cl, 17.7. Found: C, 42.3, H, 5.9, Cl, 17.5.

Reactions of II and III with $P(t\text{-Bu})_3$. (a) A solution of $P(t\text{-Bu})_3$ (0.40 mmol) in THF (5 mL) was added dropwise to a suspension of II (0.20 mmol) in THF (15 mL) at room temperature. A clear orange-red solution was obtained. Removal of the volatiles in vacuo and washing of the residue with pentane (~30 mL) gave the pale brown solid $[\text{Pt}(t\text{-Bu})_3\text{H}][\text{PtCl}_3\text{As}(t\text{-Bu})_3]$, which, even after recrystallization from dichloromethane/pentane, was found to contain traces of II. The combined filtrate and washings, on concentration, yielded a yellowish solid. Recrystallization from acetone afforded slightly impure $\text{PtCl}[\text{P}(t\text{-Bu})_2\text{CMe}_2\text{CH}_2]\text{As}(t\text{-Bu})_3$ as shown by the infrared and $^{31}\text{P}\{^1\text{H}\}$ NMR spectral measurements.

(b) Addition of $P(t\text{-Bu})_3$ (0.4 mmol) to a suspension of III (0.2 mmol) in THF (10 mL) gave a red solution. Removal of the volatiles under reduced pressure and washing of the residue with pentane (5 mL) gave red $\text{Pd}_2(\mu\text{-Cl})_2\text{Cl}_2[\text{P}(t\text{-Bu})_3]_2$: yield 85%; IR (Pd-Cl) 340 s, 315 sh, 250 s cm^{-1} .

Preparation of $\text{PtCl}[\text{P}(t\text{-Bu})_2\text{CMe}_2\text{CH}_2]\text{As}(t\text{-Bu})_3$. $\text{PtCl}[\text{P}(t\text{-Bu})_2\text{CMe}_2\text{CH}_2]_2$ (0.5 mmol) was stirred (~3 h) with $\text{As}(t\text{-Bu})_3$ (1.10 mmol) in benzene (10 mL). The solvent was removed, and the resulting product was recrystallized from hexane to give colorless plates of *trans*- $\text{PtCl}[\text{P}(t\text{-Bu})_2\text{CMe}_2\text{CH}_2][\text{As}(t\text{-Bu})_3]$ in ~90% yield (see Tables I and II).

Preparation of $[\text{P}(t\text{-Bu})_3\text{H}][\text{PtCl}_3\text{As}(t\text{-Bu})_3]$. Equimolar amounts of II and $[\text{P}(t\text{-Bu})_3\text{H}]\text{Cl}$ were stirred (~10 h) in THF at ~30 °C. Removal of the solvent and recrystallization of the residue from dichloromethane/hexane gave orange plates of $[\text{P}(t\text{-Bu})_3\text{H}][\text{PtCl}_3\text{As}(t\text{-Bu})_3]$, yield >80% (see Tables I and II).

Reaction of I with AsPh_4Cl . An equimolar mixture of I and AsPh_4Cl was stirred together in THF for ~10 h at room temperature. Removal of the solvent under reduced pressure and crystallization of the residue with dichloromethane/hexane gave orange plates of $[\text{AsPh}_4][\text{PtCl}_3\text{As}(t\text{-Bu})_3]$ in ~85% yield (see Tables I and II).

Attempted Reaction of I with $\text{CH}_2=\text{CH}_2$. Ethylene was bubbled into a solution of I in benzene for ~1 h at room temperature. There was no change in the ^1H NMR spectrum, and the removal of the volatiles afforded I quantitatively.

Attempted Reaction of I with HCl. A solution of I (0.2 mmol) in THF was stirred with HCl (0.6 mmol, produced by reacting acetyl chloride with methanol) at 0 °C for ~1/2 h. Removal of the volatiles gave unreacted I quantitatively.

Acknowledgment. Thanks are due to the National Sciences and Engineering Research Council of Canada for financial support. R.C.S. also thanks the University of Lucknow, Lucknow, India, for a leave of absence.

Registry No. I, 78610-08-9; II, 78610-09-0; III, 78610-10-3; IV, 78610-11-4; V, 78610-13-6; VI, 78610-14-7; VII, 34408-85-0; VIII, 77932-99-1; $\text{PtCl}[\text{P}(t\text{-Bu})_2\text{CMe}_2\text{CH}_2]\text{As}(t\text{-Bu})_3$, 78610-15-8; $[\text{P}(t\text{-Bu})_3\text{H}][\text{PtCl}_3\text{As}(t\text{-Bu})_3]$, 78610-17-0; *trans*- $\text{PtCl}_2(\text{PCy}_3)_2$, 60158-99-8; $\text{Pt}_2(\mu\text{-Cl})_2\text{Cl}_2(\text{PCy}_3)_2$, 76156-54-2; *trans*- $\text{PdCl}_2(\text{PCy}_3)_2$, 78655-99-9; *trans*- $\text{PtCl}_2[\text{P}(t\text{-Bu})_2\text{Ph}]_2$, 36319-68-3; $\text{Pt}_2(\mu\text{-Cl})_2\text{Cl}_2[\text{P}(t\text{-Bu})_2\text{Ph}]_2$, 78610-18-1; *trans*- $\text{PdCl}_2[\text{P}(t\text{-Bu})_2\text{Ph}]_2$, 34409-44-4; $\text{PtCl}[\text{P}(t\text{-Bu})_2\text{CMe}_2\text{CH}_2]_2$, 69393-57-3.

Contribution from the Department of Chemistry,
The University of Texas, Austin, Texas 78712

Catalytic and Structural Studies of the Rhodium(I) Complexes of the norphos and renorphos Ligands

EVAN P. KYBA,* RAYMOND E. DAVIS,* PEDRO N. JURI, and KATHLEEN R. SHIRLEY

Received May 27, 1981

Previously reported (–)-(R,R)-2-*exo*-3-*endo*-bis(diphenylphosphino)bicyclo[2.2.1]heptene (norphos) and its reduced congener (–)-(R,R)-2-*exo*-3-*endo*-bis(diphenylphosphino)bicyclo[2.2.1]heptane (renorphos) have been studied as chiral ligands for the Rh(I)-catalyzed reductions of prochiral substrates. It was found that reduction of the norphos to renorphos ligand occurs upon catalyst activation so that the ligand on the operating catalyst is renorphos, regardless of the precursor. High hydrogenation *ee*'s (95%) were obtained with two enamide substrates but only moderate (63%) for itaconic acid. Crystal structure data at –100 °C: *a* = 15.765 (8) Å, *b* = 20.482 (9) Å, *c* = 11.317 (4) Å, orthorhombic, $P2_12_1$ (No. 16), *Z* = 4, *R* = 0.047, *R_w* = 0.048, absolute configuration determined, 3944 reflections with *I* > 2.5 σ _{*I*}. X-ray data were collected at –100 °C on a Syntex P2₁ autodiffractometer with monochromated Mo K α radiation. The norphos ligand chelates the Rh(I) center although it must suffer severe distortions in order to do so. The largest distortion is the change in dihedral angle PCCP from 120 to 64°. The bicyclo[2.2.1]heptene skeleton absorbs this drastic change in dihedral angle in smaller changes in dihedral and bond angles, as well as bond lengths.

There is extant a large amount of published work dealing with the design and synthesis of chiral diphosphines as ligands for transition metals [mainly Rh(I)] for asymmetric induction during catalytic transformations of organic molecules.¹ By

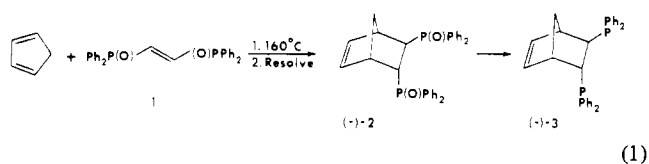
far the most studied catalytic reaction is hydrogenation of enamides to give amino acid derivatives, and recent work by the Halpern,² Brown,³ and Ojima^{4a-c} groups has led to a good

(1) (a) Valentine, D., Jr.; Scott, J. W. *Synthesis* 1978, 329. (b) Glaser, R.; Geresh, S.; Twaik, M. *Isr. J. Chem.* 1980, 20, 102.

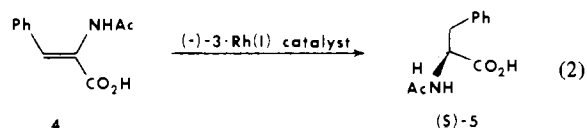
(2) (a) Chan, A. S. C.; Pluth, J. J.; Halpern, J. *J. Am. Chem. Soc.* 1980, 102, 5952 and references contained therein. (b) Chan, A. S. C.; Halpern, J. *Ibid.* 1980, 102, 838.

understanding of the details of the mechanism of asymmetric induction in such processes.

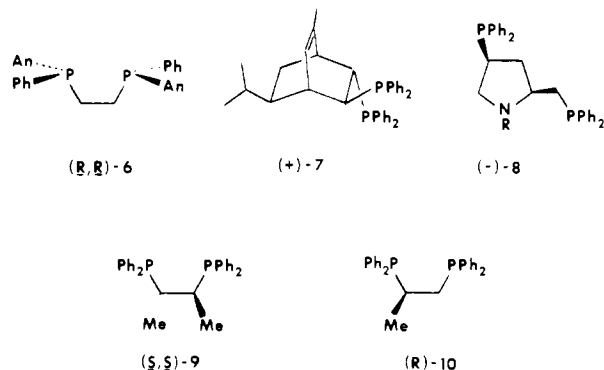
Recently, Brunner and Pieronczyk described the synthesis of optically active (+)- and (-)-norphos (**3**, eq 1) which they



used as a ligand for Rh(I) in effecting the asymmetric reduction of (*Z*)- α -acetamidocinnamic acid (**4**) to *N*-acetylphenylalanine (**5**) in high optical yields (eq 2).⁵ They touted



the bidentate ligand **3** as one of the most easily prepared, and one which gives among the highest inductions of asymmetry during catalytic hydrogenation of **4**, rivaled only by the Monsanto group's dipamp (**6**),⁶ Kagan's phellaphos (**7**),⁷ and the Achiwa-Ojima ligand (**8**).⁴



Brunner suggested that **3** is a chelating diphosphine as are other 1,2-diphosphinoethanes such as **6**, chiraphos (**9**),⁸ and prophos (**10**).⁹ Examination of Dreiding models of **3** reveals that, unlike the freely rotating **6**, **9**, and **10**, the phosphino sites are locked with the dihedral angle P-C-C-P at 120°. Study of Dreiding models of **3** chelated to an octahedral or square-planar metal atom shows that the chelate ring will not tolerate a dihedral angle (PCCP) of 120° and that, in order to form the chelate, severe distortions must be imposed on the rigid [2.2.1] skeleton. The question thus arose as to whether or not the energy cost of [2.2.1] skeletal distortion would be offset by that gained upon chelation of a Rh(I) species. It appeared possible that a more comfortable chiral chelate could be formed with the use of the *endo*-PPh₂ and the *endo* face of the double bond. On the other hand, the double bond might not survive the reductive reaction conditions and the operating

Table I. Selected Physical Data for norphos (**3**), renorphos (**12**), and Their (Norbornadiene)rhodium Perchlorate Complexes

	mp, °C	$[\alpha]_{\lambda}^{25}$, deg (c, solvent) ^a	³¹ P NMR, ppm ^b
(-)- 3	130-131	-43.6 (0.55, CHCl ₃)	-1.2, -3.0 ^c
(-)- 12	95-97	-41.8 (1.72, CHCl ₃)	1.6, -9.7 ^c
(-)- 15	210 (dec)	-104.5 (0.30, MeOH)	25.8, 24.9 ^d
(+)- 16	230 (dec)	+110.0 (0.11, MeOH)	37.3 (dd), 26.1 (dd) ^e

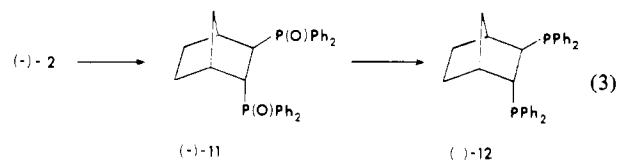
^a Optical rotation for **3** and **12** measured at $\lambda = 578$ nm and for **15** and **16** at $\lambda = 589$ nm. ^b Chemical shifts downfield from external 85% H₃PO₄ are defined as positive. ^c CDCl₃ solution (10% w/v). No P-P coupling evident. ^d CDCl₃/EtOD (1/1 v/v), second-order spectrum: $J_{P_1, P_2} = 20$ Hz, $J_{P_1, Rh} = J_{P_2, Rh} = 150$ Hz. ^e MeOD solution (5% w/v): $J_{P_1, P_2} = 32$ Hz, $J_{P_1, Rh} = J_{P_2, Rh} = 157$ Hz.

ligand might involve the norbornane rather than the norbornene skeleton. Because of these questions and others described below, we have investigated in detail the properties of **3** and its reduced congener **12** vis-à-vis coordination of Rh(I) and the asymmetric reduction ability of such Rh(I) complexes.

Results

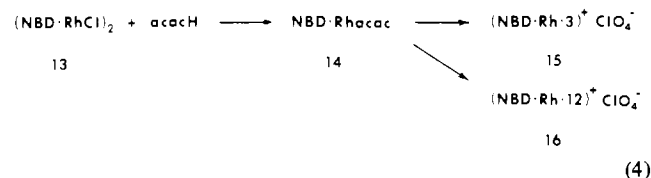
Synthesis of Chiral Ligands. (-)- and (+)-norphos (**3**) were synthesized as shown in eq 1. The Diels-Alder reaction of cyclopentadiene and **1** gave (+)-**2** in 76% yield with the use of a modified published procedure.¹⁰ It should be noted that if the reaction temperature exceeds ca. 170 °C for a significant length of time, a substantial amount of a side product, which we believe to be the Diels-Alder adduct of **2** and cyclopentadiene, is formed. The facile resolution of (+)-**2** using (-)-dibenzoyltartaric acid gave (-)-**2** (70% of the available (-) isomer) and (+)-**2** (50%, using (+)-dibenzoyltartaric acid on the mother liquors). Reduction of (-)-**2** to (-)-**3** was carried out according to Brunner, using trichlorosilane.^{5,11}

The double bond in (-)- or (+)-**2** was reduced to give (-)- or (+)-**11** (80%) with use of diimide generated from the thermal decomposition of *p*-toluenesulfonylhydrazide in boiling glyme (eq 3).¹² Trichlorosilane reduction of (-)- or (+)-**11**



gave (-)- or (+)-**12** [(-)- or (+)-renorphos] in yields of 70-80%. Selected physical data concerning **3** and **12** are presented in Table I.

Synthesis of Chiral Rh(I) Catalyst Precursors. The crystalline cationic norbornadiene diphosphine rhodium(I) perchlorates **15** and **16** were prepared as shown in eq 4. The



norbornadiene rhodium chloride dimer (**13**) was prepared according to Wilkinson,¹³ and this was converted into the acetylacetonate **14** with the use of a procedure similar to that described by Cramer.¹⁴ The chiral diphosphine complexes

- (3) (a) Brown, J. M.; Parker, D. *J. Chem. Soc., Chem. Commun.* **1980**, 342. (b) Brown, J. M.; Chaloner, P. A. *Ibid.* **1980**, 344. (c) Brown, J. M.; Chaloner, P. A. *J. Am. Chem. Soc.* **1980**, *102*, 3040. (4) (a) Ojima, I.; Kogure, T.; Yoda, N. *J. Org. Chem.* **1980**, *45*, 4728; (b) Ojima, I.; Kogure, T.; Yoda, N. *Chem. Lett.* **1979**, 495. (c) Ojima, I.; Kogure, T. *Ibid.* **1979**, 641. (d) Achiwa, K. *J. Am. Chem. Soc.* **1976**, *98*, 8265. (5) Brunner, H.; Pieronczyk, W. *Angew. Chem., Int. Ed. Engl.* **1979**, *18*, 620. (6) Vineyard, B. D.; Knowles, W. S.; Sabacky, M. J.; Bachman, G. L.; Weinkauff, D. J. *J. Am. Chem. Soc.* **1977**, *99*, 5946. (7) Lauer, M.; Samuel, O.; Kagan, H. B. *J. Organomet. Chem.* **1979**, *177*, 309. (8) Fryzuk, M. D.; Bosnich, B. *J. Am. Chem. Soc.* **1977**, *99*, 6262. (9) Fryzuk, M. D.; Bosnich, B. *J. Am. Chem. Soc.* **1978**, *100*, 5491.

- (10) Nesterova, N. P.; Medved, T. Y.; Polikarpov, Y. M.; Kabachnik, M. I. *Bull. Acad. Sci. USSR, Div. Chem. Sci. (Engl. Transl.)* **1974**, *23*, 2210. (11) Naumann, K.; Zon, G.; Mislow, K. *J. Am. Chem. Soc.* **1969**, *91*, 7012. (12) Dewey, R. S.; van Tamelen, E. E. *J. Am. Chem. Soc.* **1961**, *83*, 3729. (13) Abel, E. W.; Bennett, M. A.; Wilkinson, G. *J. Chem. Soc.* **1959**, 3178.

were then obtained in yields of about 65% from **14** and **3** or **12** in THF in the presence of perchloric acid.^{8,15} Examination by ³¹P NMR spectroscopy of the mother liquors from which **15** and **16** crystallized revealed a complex absorption pattern, indicative of a mixture of components.

This technique gives **15** and **16** as ruby red X-ray quality crystals which appear to be indefinitely air stable. In an alternative preparation, the dropwise addition of aqueous sodium perchlorate to a methanolic solution of either **3** or **12** plus **13** gave **15** or **16**, respectively, as orange powders in yields in excess of 90%.¹⁶ Although the physical appearance of the complexes obtained this way differed from those obtained from **14**, the spectroscopic properties of the complexes obtained by either method were identical (see Table I for ³¹P NMR data).

Asymmetric Catalytic Hydrogenation of (Z)- α -Acetamidocinnamic Acid. Preparative experiments were carried out in degassed methanol solutions. The rhodium catalyst precursor (ca. 0.01 mmol) was dissolved in the alcoholic solvent (3 mL) and then stirred under a hydrogen atmosphere for 1 h. The substrate **4** (0.9 mmol) in degassed methanol (3 mL) was then added by syringe; hydrogenation was effected at 1.6 atm and was complete in about 1 h. At the end of the reaction, methanol was removed by rotary evaporation and the rhodium catalyst was removed by treatment of the residue with aqueous sodium hydroxide for 2 h followed by filtration. The basic aqueous filtrate was acidified to pH 2 with 1 M HCl and then extracted with ether. Optical rotation measurements were performed on the crude **5** obtained by concentration of the ethereal extracts. Alternatively, the reaction mixture was stirred with a strongly acidic ion-exchange resin, filtered, and concentrated, and the rotation of the solid residue was determined. The reduction of **4** mediated by either (-)-**15** or (-)-**16** gave (+)-(*S*)-**5** with $[\alpha]_D^{25} 45.1 \pm 0.1^\circ$, which corresponds to 95% ee.¹⁷ It should be noted also that in situ catalyst preparation from **13** and (-)-**3** or (-)-**12** gave optical yields identical with those employing (-)-**15** or (-)-**16**. Reduction of **4** at elevated pressures (65–70 atm H₂) gave enantiomeric excesses in **5** in the range of 30% with (+)-**16**. The same result was obtained with (-)-**15**.

Crude kinetic studies were performed on reductions of **4** and **5** using catalysts from (-)-**3**, (-)-**12**, and diphos (Ph₂PCH₂CH₂PPh₂). The rates of reduction as followed by uptake of dihydrogen at 1.6 atm were identical for the two chiral ligands [27 mol of H₂ (mol of catalyst)⁻¹ h⁻¹] when in situ catalysts were generated from cyclooctadienerrhodium chloride dimer and the diphosphine. The diphos catalyst was twice as fast (58 mol of H₂ (mol catalyst)⁻¹ h⁻¹). The cationic complexes **15**, **16**, and (diphos)Rh(NBD)ClO₄ gave hydrogenation rates 1–2 times greater than the in situ catalysts, and the diphos catalyst was about three times faster than these derived from **15** or **16** (310 vs. 98 mol of H₂ (mol catalyst)⁻¹ h⁻¹, respectively).

The catalyst generation and reduction of **4** was followed with use of ³¹P NMR spectroscopy. Equation 6 shows the stages at which spectra were determined for both (-)-**15** and (+)-**16**. The catalyst precursor was dissolved in MeOD under an argon atmosphere and spectrum 1 was determined (Figure 1). This solution was then stirred under hydrogen for 0.5 h, and spectrum 2 was run after replacing the hydrogen with argon. Spectrum 3 was obtained after **4** was added under an argon atmosphere to the reduced catalyst precursor. Finally spec-

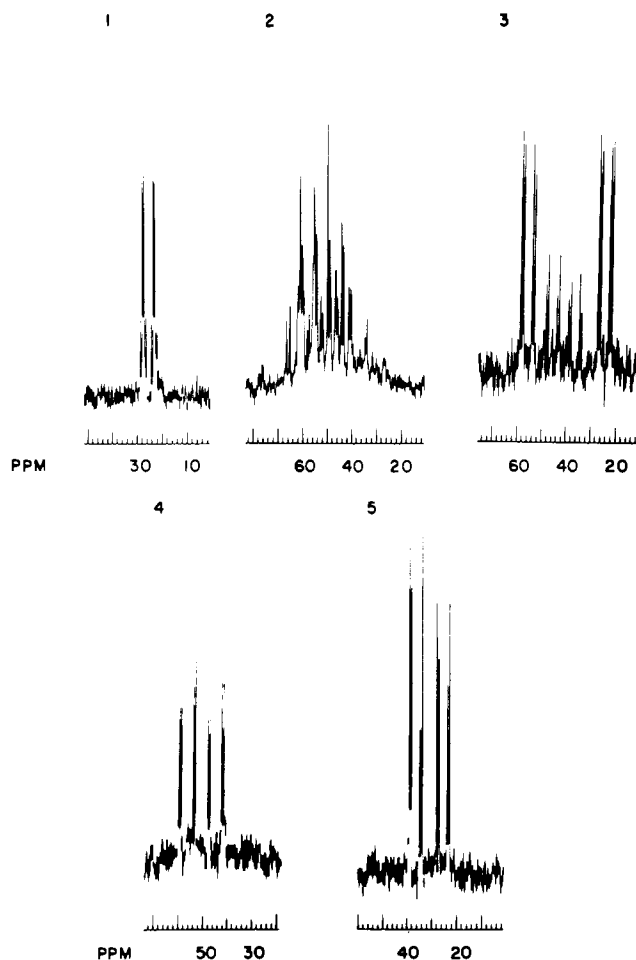


Figure 1. ³¹P NMR spectra of hydrogenation catalyst precursors (-)-**15** and (+)-**16** at various stages of reaction. Equation 6 describes the history of the sample prior to each spectrum. Note that spectra 6–8 referred to in eq 6 are not shown.

Table II. Hydrogenation Data for Enamide Substrates

run no.	catalyst ^a	substrate ^a	product ^b	(config)	turn-over ^e	% ee ^d
1	(-)- 15	4	(+)- 5	(<i>S</i>)	85	95
2	(+)- 16	4	(-)- 5	(<i>R</i>)	111	95
3	21	4	5		317	
4	diphos ^c	4	5		49	
5	(+)- 16	17	(+)- 18	(<i>R</i>)	784	95
6	(+)- 16	19	(-)- 20	(<i>S</i>)	312	63
7	21	4	5		300	
8	diphos ^c	4	5		406	

^a For runs 1–4 and 6: [catalyst] = 1.56×10^{-3} M, [substrate] = 1.30×10^{-1} M. For run 5: [catalyst] = 4.7×10^{-4} M, [substrate] = 3.9×10^{-2} M. For runs 7 and 8: [catalyst] = 7.2×10^{-4} M, [substrate] = 6.0×10^{-2} M. ^b Reaction completion checked by ¹H NMR. ^c Catalyst generated in situ in the presence of (NBDRhCl)₂. ^d Based on reported maximum rotations: *N*-acetyl-(*S*)-phenylalanine, $[\alpha]_D^{20} +47.4^\circ$ (c 1.0, 95% EtOH);⁶ *N*-acetyl-(*R*)-alanine, $[\alpha]_D^{36} +66.3^\circ$ (c 2.0, H₂O);⁸ (*R*)-methylsuccinic acid, $[\alpha]_D^{20} +17.01$ (c 4.41, EtOH) (Rossi, R. *Gazz. Chim. Ital.* 1968, 98, 1391). ^e Moles of H₂ per mole of catalyst per hour.

trum **4** was taken after substrate **4** had been completely reduced, as evidenced by the change in color of the solution from deep red to pale orange. Figure 1 shows the spectra taken at these four stages for (-)-**15** as well as spectrum 5 for (+)-**16**. Spectra 6–8 for (+)-**16** were identical with 2–4, respectively, for (-)-**15**.

Finally, we have evaluated the optical induction efficacy of **16** with regard to reduction of two other substrates, **17** → **18**

(14) Cramer, R. *J. Am. Chem. Soc.* 1964, 86, 217.

(15) Schrock, R. R.; Osborn, J. A. *J. Am. Chem. Soc.* 1971, 93, 2397.

(16) King, R. B.; Bakos, J.; Hoff, C. D.; Markó, L. *J. Org. Chem.* 1979, 44, 1729.

(17) For optically pure (*S*)-**5**, $[\alpha]_D^{20} +47.4^\circ$ (c 1.0, 95% EtOH) was used.⁶ A somewhat lower value (+46.8°) has been used by others, including, apparently: Brunner;⁵ Gelbard, G.; Kagan, H. B.; Stern, R. *Tetrahedron* 1976, 32, 233.

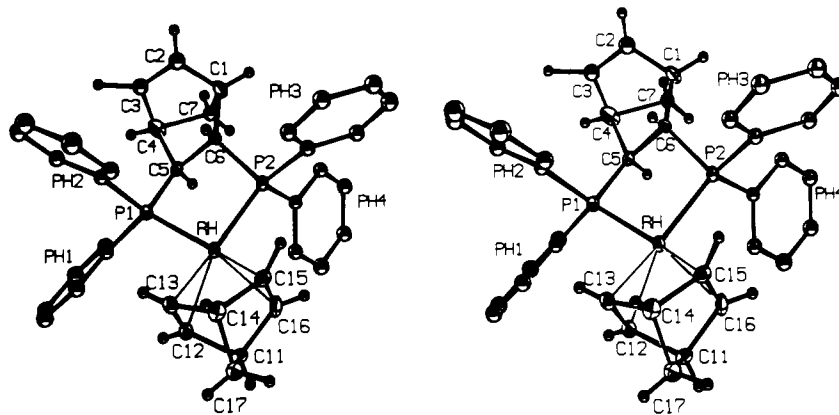
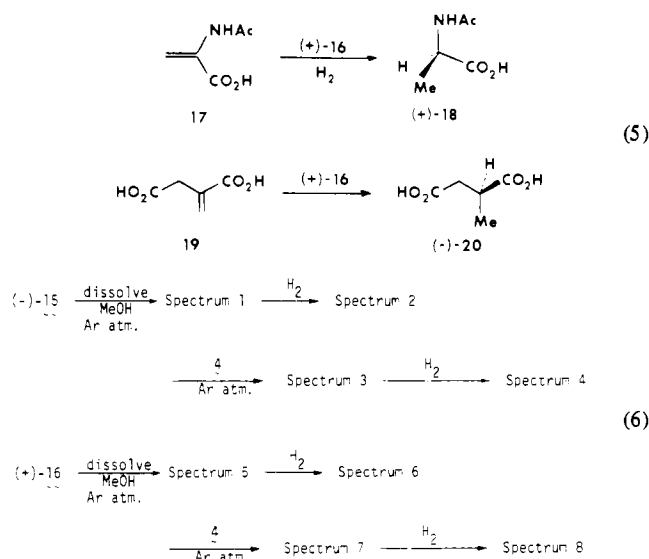


Figure 2. Stereoscopic view of the cation of **15**, illustrating the atom numbering scheme used in the crystallographic presentation and discussion. The disordered atoms C2, C3, and C7 are shown in their A positions (Table IV), which are statistically 50% occupied in the crystal. Equiprobability ellipsoids or spheres of 30% probability are shown for nonhydrogens; hydrogens are represented as 0.25-Å spheres.

and **19** → **20** (eq 5), which gave 95 and 63% ee's, respectively. Relative rates of hydrogenation are given in Table II.



Discussion

Chiral Catalyst Operation. Information concerning the chelating nature of the ligands **3** and **12** was obtained from the ^{31}P NMR spectra of **15** and **16**, which are shown in Figure 1 (1 and 5). The spectrum due to **16** was first order, with the three coupling constants $J_{\text{P}_x\text{P}_y}$, $J_{\text{P}_x\text{Rh}}$, and $J_{\text{P}_y\text{Rh}}$ ($\text{P}_x = \text{exo-P}$, $\text{P}_y = \text{endo-P}$) directly extractable from it (Table I). In contrast, the spectrum of **15** was a deceptively simple second-order one, which could be reproduced easily by calculation¹⁸ to yield the chemical shifts and coupling constants given in Table I. It is clear from these data that the norphos ligand is chelating the rhodium center via the two phosphorus sites, and we present below an X-ray structure determination of **15** which reveals the distortions from normal bond angles and lengths as a consequence of chelation.

It has been noted that five-membered chelates of diphos-type ligands exhibit unusually large ^{31}P NMR coordination chemical shifts [$\Delta_p = \delta(\text{complex}) - \delta(\text{free})$] in a variety of metal complexes.¹⁹ Although ring strain has been suggested as the cause for this phenomenon,^{19a} it is clear that the situation is more complex.^{19b,d} Generally, these coordination chemical

shifts, Δ_p , are in the range of 59–68 ppm for chelates of the type $(\text{NBD})\text{Rh}(\text{PCCP})^+$ and are about 25–30 ppm larger than for corresponding nonchelates.²⁰ Ligand **3** appears to be the only one which does not exhibit this large downfield coordination shift ($\Delta_p = 26, 28$ ppm), and the somewhat less rigid **12** also has an attenuated coordination shift ($\Delta_p = 35, 36$ ppm). Whatever the five-membered chelate deshielding effect is due to, apparently it is offset by imposing a strain on the chelate.

The fact that ^{31}P NMR spectra 2–4 (Figure 1) are identical for catalysts $(-)\text{-15}$ and $(+)\text{-16}$ reveals that hydrogenation of the NBD ligand in $(-)\text{-15}$ results also in reduction of the norbornene to the norbornane skeleton of the diphosphine ligand. Thus in the working catalyst, the chiral ligand is the renorphos (**12**) species regardless of the precursor. Spectra 1–4 are similar to those reported by Brown and Chaloner,^{3c} although the isomers (ratio 7:3) giving rise to spectrum 3 might be diastereomeric or geometric (carbonyl trans to each of the inequivalent phosphorus atoms).²¹ Baird and his co-workers²⁰ have observed also a pair of isomers with $(R)\text{-10}$, which has inequivalent phosphorus atoms. In view of the observation that only one diastereomer is observed with chiraphosphorhodium complexes of enamides of the type exemplified by **4**,^{2a,3c,20} as well as our finding (vide infra) that there exists a pseudo- C_2 axis relating the exo- and endo-P atoms in **15**, it seems quite likely that the isomers giving rise to the two sets of eight peaks in spectrum 3 are geometrical.

Since optically active **3** was obtained by a resolution in which the chirality could only be assumed on the basis of asymmetric hydrogenation data,⁵ we have used anomalous dispersion studies (Experimental Section) to show that $(+)\text{-3}$ is the S,S isomer, confirming Brunner's original assignment.⁵ Thus the chirality of the diphosphine relative to the amino acid derivative produced is the same for **3**, **12**, **9**, and **10**.

Our observation that the **17** → **18** transformation occurs with high enantioselectivity is indicative that the renorphos ligand may effect generally high asymmetric induction with such amino acid precursors. On the other hand, the renorphos ligand is not nearly as effective as the Achiwa–Ojima ligand **8** ($R = \text{OCOBu-}t$) in reducing itaconic acid (**19**), with $(+)\text{-12}$ giving only 63% ee compared to 91% for **8**.^{4a}

Structure of (norphos)Rh(NBD)ClO₄ (15**).** Our interest in this species was heightened following the study of Dreiding models which indicated that the five-membered chelate ring should be strained due to the "natural" PCCP dihedral being 120°. Since the norbornene skeleton is one of the most rigid in organic chemistry, it was of interest to see how the strain in the chelate ring would be played off against distortions in

(18) "NMRCAL", Nicolet NIC-05-40417.

(19) (a) Connor, J. A.; Day, J. P.; Jones, E. M.; McEwen, G. K. *J. Chem. Soc., Dalton Trans.* **1973**, 347. (b) Grim, S. O.; Briggs, W. L.; Barth, R. C.; Tolman, C. A.; Jesson, J. P. *Inorg. Chem.* **1974**, *13*, 1095. (c) Garrou, P. E. *Ibid.* **1975**, *14*, 1435. (d) Kyba, E. P.; Brown, S. B. *Ibid.* **1980**, *19*, 2159.

(20) Slack, D. A.; Greveling, I.; Baird, M. C. *Inorg. Chem.* **1979**, *18*, 3125.

(21) We thank a reviewer for alerting us to this point.

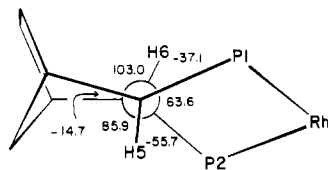


Figure 3. Newman projection illustrating the torsion angles about the C5–C6 bond. As in the other figures, the disordered atoms C2, C3, and C7 are shown in the A positions.

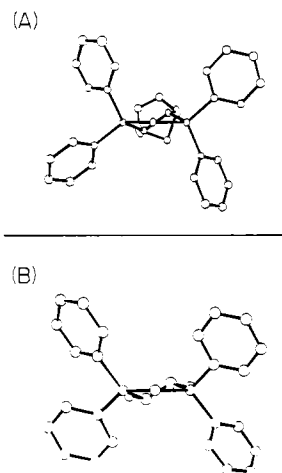


Figure 4. Perspective view of (A) **15** and (B) **22** along the bisector of the P–Rh–P bond, omitting the diene ligand in each case.

the bicyclo[2.2.1]hept-2-ene skeleton. As can be seen from stereoview (Figure 2) and the perspective view in Figure 3, as well as from the data in Table VI, the “natural” dihedral angle of 120° has been closed to 64° . In fact, comparison of the geometrical properties of the chelate ring in **15** with that of the corresponding (chiraphos)Rh(COD) (**22**) complex²² (Figure 4) reveals the largest difference to be this dihedral angle 64° (cf. 52°). This distortion is accommodated in the chelate ring as evenly as possible by adjustments in other dihedral and bond angles and, to a lesser extent, even in bond lengths. Thus the more limited flexibility of the chelate ring in **15** compared to that in **22** results in the former having smaller C–P–Rh angles (103.8 and 103.3° vs. 109.5 and 110.1°), longer P–Rh bonds (2.323 and 2.321 Å vs. 2.275 and 2.266 Å), and a larger P–Rh–P angle (86.4 vs. 83.8°). This pattern of differences suggests, then, that in **15** the constraints on the phosphorus atom orientations result in less strong P–Rh bonding.

It appears that the [2.2.1] skeleton also is deformed by the strain of the dihedral distortion about the C5–C6 bond. A comparison of structural parameters of **15** with those of well-determined undistorted [2.2.1] ring systems reveals a series of small but consistent alterations in bond angles, concentrated predominantly in the five-membered ring C1–C7–C6–C5–C4. However, a detailed discussion of these accommodations is not felt to be warranted because of the disorder in the crystal, by which the 1,2-ethylidene bridge and the methylene bridge are randomly distributed in the crystal structure (vide infra).

It is generally felt that the transfer of chirality from the catalyst to the substrate during the hydrogenation process is a consequence of the chiral array of the four phosphine phenyl groups which occupy pseudoaxial and -equatorial positions in the chelate.⁸ The substituents on the carbon supporting framework, e.g., the methyl or methyls on **9** and **10**, the cyclopentene (**3**), cyclopentane (**12**), or cyclohexene (**7**) appendages, enforce a chiral conformation which in turn gen-

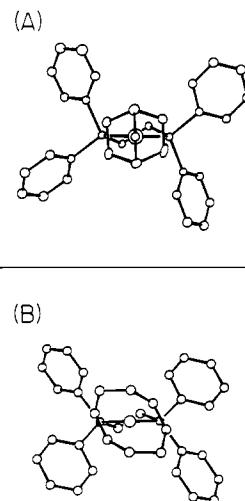


Figure 5. Perspective view of (A) **15** and (B) **22** as in Figure 4, but omitting the noncholate atoms of the phosphine ligand. Note the significant skewing of the diene ligand in each case.

erates the chiral arrangement of phenyl groups. Figure 4, which compares ORTEP plots of **22**²² and **15**, illustrates this notion very nicely. Thus from a vantage point in front of the rhodium atom with the diene ligands not shown, the pseudoaxial and -equatorial positions of the phenyl groups are evident in both **15** and **22** but are more pronounced in the former. In both cases the diene ligand is rotated away from an orientation which would place the double bonds perpendicular to the PRhP plane, and in both cases the sense of this rotation is counterclockwise, with much more internal distortion occurring in the more flexible COD ligand of **22** (Figure 5). The forces which cause this nonideal diene orientation, be they steric or electronic, presumably would be those which would lead to enantioface differentiation in a prochiral olefin.

Conclusion

The optically active norphos ligand functions as a precursor to the renorphos ligand in the Rh(I)-catalyzed asymmetric hydrogenations of prochiral olefins. The renorphos ligand is excellent in inducing asymmetry in enamide precursors of amino acid derivatives ($\geq 95\%$ ee) but only moderate for itaconic acid (63% ee). The X-ray structure determination of **15** has established unambiguously that (+)-norphos is the *S,S* isomer, and that the strain of forming the norphos–rhodium chelate is dispersed throughout the chelate as well as the supporting norbornene skeleton.

Experimental Section

General Data. Melting points were obtained with the use of a Thomas-Hoover capillary melting point apparatus and are uncorrected. Elemental analyses were performed by Chemalytics, Inc., Tempe, AZ, or Galbraith Laboratories, Inc., Knoxville, TN.

Infrared spectra (IR) were recorded on a Perkin-Elmer 237B grating spectrophotometer.

Proton magnetic resonance spectra (^1H NMR) were obtained on Varian EM-390, Nicolet NT-200 or Varian HA-100 instruments. Chemical shifts are given in δ downfield from tetramethylsilane, and coupling constants are reported in hertz. Multiplicities are as follows: s = singlet, d = doublet, t = triplet, q = quartet, m = multiplet. Carbon-13 and phosphorus-31 NMR spectra were determined on a Bruker instrument at 22.6 and 36.4 MHz, respectively. Chemical shifts are given as parts per million (ppm) relative to Me_4Si for ^{13}C NMR and relative to 85% H_3PO_4 for ^{31}P NMR spectra. Chemical shifts upfield from 85% H_3PO_4 are defined as negative for the ^{31}P spectra. The ^{13}C and ^{31}P NMR spectra are proton decoupled.

Mass spectra were determined on a CEC-21-100 high-resolution instrument or a Du Pont 21-491 instrument at 70 eV.

Gas chromatographic analyses were performed on either a Varian-Aerograph 2720 (thermal conductivity detector) or 2740 (flame ionization detector) instrument using either 5% or 20% SE-30 on Gas

Table III. Crystallographic Summary for $15 \cdot C_4H_8O$

A. Crystal Data at $-100^\circ C^a$	
$a = 15.765$ (8) Å	fw = 829.11
$b = 20.482$ (9) Å	$d_{\text{calc}} = 1.367$ g/cm ³
$c = 11.317$ (4) Å	$d_{\text{meas}}^b = 1.45$ g/cm ³
crystal system: orthorhombic	$Z = 4$
space group: $P2_12_1$ (No. 16)	$F(000) = 649$
B. Collection at $-100^\circ C$ and Processing of Intensity Data	
Syntax P2 ₁ autodiffractometer equipped with graphite monochromator and Syntax LT-1 low-temperature gas (N ₂) delivery system	
radiation: Mo K α , $\lambda = 0.71069$	
mode: ω scan	
scan range: $4-55^\circ$	
bkgd: offset 1.0° and -1.0° in ω from $K\alpha_{1,2}$ maximum	
scan rate: variable, $2.5-5^\circ/\text{min}$	
2θ range: $4-55^\circ$	
reflectns measd: 4681	
check reflections: 4 reflections— $(\bar{2}40)$, $(04\bar{2})$, (312) , (400) —remeasured after every 96 reflections; analysis ^c of these data revealed no significant decay of the crystal	
data crystal dims: $0.28 \times 0.16 \times 0.50$ mm	
data crystal volume: 0.0157 mm ³	
absn coeff (THF not included), μ (Mo K α): 6.61 cm ⁻¹	
transmission factor range: $0.855-0.916$	

^a Unit cell parameters were obtained by least-squares refinement against the observed setting angles of 45 locally intense reflections with $25.1^\circ < 2\theta < 26.6^\circ$. ^b Flotation, aqueous NaClO₄. ^c Henslee, W. H.; Davis, R. E. *Acta Crystallogr., Sect. B* 1975, B31, 1511.

Table IV. Fractional Coordinates for Nongroup Nonhydrogen Atoms^a

atom	x	y	z
RH ^b	83978 (3)	85629 (2)	82789 (4)
P1 ^b	88824 (10)	74928 (7)	82939 (16)
P2 ^b	92749 (11)	87293 (7)	98975 (14)
C1	10678 (5)	7785 (3)	10746 (7)
C2A	11200 (10)	7328 (7)	10163 (14)
C2B	10357 (10)	7477 (8)	11745 (16)
C3A	10756 (9)	6799 (7)	9885 (13)
C3B	9970 (10)	6921 (8)	11424 (13)
C4	9978 (6)	6856 (3)	10261 (8)
C5	9398 (4)	7413 (3)	9724 (5)
C6	9977 (4)	8018 (3)	9871 (6)
C7A	10104 (9)	7248 (8)	11549 (13)
C7B	10940 (10)	7167 (7)	9917 (13)
C11	6849 (4)	9133 (3)	7652 (6)
C12	7218 (4)	8472 (3)	7282 (6)
C13	7851 (4)	8593 (3)	6496 (5)
C14	7915 (5)	9353 (3)	6367 (6)
C15	8233 (4)	9565 (3)	7587 (6)
C16	7583 (5)	9441 (3)	8366 (7)
C17	6965 (5)	9523 (3)	6501 (7)
Cl ^b	101782 (15)	99619 (9)	149602 (21)
O2	9436 (5)	10164 (4)	14475 (11)
O3	10171 (5)	9294 (3)	15189 (10)
O4	10353 (9)	10285 (4)	15955 (8)
O5	10774 (10)	10166 (6)	14195 (12)

^a See Figure 2 for identity of the atoms; Cl, O2, O3, O4, O5 are the atoms in the perchlorate ion. Numbers in parentheses are estimated standard deviations in the units of the last significant digit for the parameter. ^b For Rh, P, and Cl atoms, values are presented $\times 10^5$.

Table V. Rigid Group Parameters for Phenyl Rings^a

ring	P atom	x_0	y_0	z_0	ϕ	θ	ρ
PH1	P1	0.8118 (2)	0.6831 (2)	0.8131 (3)	5.557 (3)	-2.995 (2)	-1.968 (3)
PH2	P1	0.9651 (3)	0.7325 (2)	0.7134 (3)	1.269 (3)	-2.288 (3)	2.759 (4)
PH3	P2	0.9956 (2)	0.9450 (2)	0.9878 (4)	2.446 (3)	-3.067 (2)	1.275 (3)
PH4	P2	0.8709 (2)	0.8715 (2)	1.1294 (3)	4.690 (4)	2.132 (2)	1.628 (4)

^a A description of these group parameters is provided elsewhere.²⁷ Angular coordinates are in radians. The internal coordinate system of a phenyl ring has been defined previously.²⁸

Chrom Q, packed in stainless-steel columns (6 ft by 0.188 in. or 6 ft by 0.125 in.). Peak area measurements were obtained with the aid of a Vidar 6300 digital integrator.

X-ray measurements were performed on a Syntax P2₁ autodiffractometer.

Unless noted, all of the reactions, manipulations, and purification steps involving phosphines and solutions of rhodium species were performed under a dry nitrogen or argon atmosphere. Air-sensitive liquids were transferred by Teflon flexneedles with the use of nitrogen pressure or by syringe. All concentrations of solutions were carried out on a rotary evaporator under water aspirator pressures unless otherwise noted. Solutions were dried with anhydrous magnesium sulfate.

The following compounds were prepared according to literature procedures with little or no modifications: (*E*)-1,2-bis(diphenylphosphoryl)ethylene (1), (-)-5-*exo*-6-*endo*-bis(diphenylphosphoryl)bicyclo[2.2.1]hept-2-ene (2),¹⁰ (-)-5-*exo*-6-*endo*-bis(diphenylphosphino)bicyclo[2.2.1]hept-2-ene (3),^{5,11} bis(norbornadiene)- μ,μ' -dichlorodirrhodium (13),¹³ (norbornadiene)rhodium acetylacetonate (14),¹⁴ and (1,2-bis(diphenylphosphino)ethane)-(norbornadiene)rhodium perchlorate.¹⁵

(-)-(*R,R*)-2-*exo*-3-*endo*-Bis(diphenylphosphoryl)bicyclo[2.2.1]heptane (11). *p*-Toluenesulfonylhydrazide (5.0 g, 26.8 mmol) and (-)-2 (1.61 g, 3.2 mmol) were reacted in boiling 1,2-dimethoxyethane (70 mL) for 72 h. The hot solution was filtered and concentrated, and the residue was partitioned between chloroform (30 mL) and 2% aqueous potassium hydroxide (40 mL). The aqueous layer was extracted with chloroform (2×20 mL), and the combined organic extracts were dried and concentrated to give a white solid. This was recrystallized from acetone to give (-)-11 as a white solid (1.16 g, 72%): mp $285^\circ C$ dec; $[\alpha]_D^{25} -70.0^\circ$ (c 2.01, CHCl₃); ¹H NMR (CDCl₃) δ 7.9–6.8 (complex m, 20 H), 3.9–1.1 (complex m, 10 H); ³¹P NMR (CDCl₃) δ 32.1 (d, $J_{PP} = 11$ Hz), 29.3 (d, $J_{PP} = 11$ Hz); mass spectrum m/e 496 (M^+).

(-)-(*R,R*)-2-*exo*-3-*endo*-Bis(diphenylphosphino)bicyclo[2.2.1]heptane (12). A solution of (-)-11 (1.02 g, 2.06 mmol) and trichlorosilane (6.4 g, 47 mmol) in benzene (20 mL) was heated in a sealed tube at $80^\circ C$ for 23 h. The cooled reaction mixture was diluted with benzene (20 mL) and then quenched by the dropwise addition of 25% aqueous sodium hydroxide (100 mL). The organic layer was washed with water (2×20 mL), dried, and concentrated to give a colorless oil, which solidified upon addition of acetone. The solid was recrystallized from acetone to give 12 as a white solid (684 mg, 72%): mp $95-97^\circ C$; $[\alpha]_D^{25} -42.6^\circ$ (c 0.713, CHCl₃), $[\alpha]_{578}^{25} -41.8^\circ$ (c 1.72, CHCl₃); ¹H NMR (CDCl₃) δ 7.7–7.0 (complex m, 20 H), 2.4–0.3 (complex m, 10 H); ³¹P NMR (CD₂Cl₂) δ 1.6 (s), -9.7 (s).

Anal. Calcd for C₃₁H₃₀P₂: C, 80.17; H, 6.46. Found: C, 79.94; H, 6.62.

(-)-(norphos)(norbornadiene)rhodium Perchlorate (15) and (+)-(renorphos)(norbornadiene)rhodium Perchlorate (16). To a solution of (norbornadiene)rhodium acetylacetonate (72.3 mg, 0.24 mmol) and (-)-norphos (114 mg, 0.24 mmol) in THF (2 mL) was added 70% aqueous perchloric acid (35 mg, 0.24 mmol) in THF (0.5 mL). The resultant deep red solution was allowed to stand at room temperature for 48 h and then filtered to give 15 as ruby red crystals (130 mg, 64%): mp $185^\circ C$ dec; ³¹P NMR (CDCl₃/EtOD, 1/1, v/v) δ 25.8 (4 lines), 24.9 (4 lines), second-order spectrum computer fitted¹⁸ to give $J_{PP} = 20$ Hz, $J_{P,Rh} = J_{P_2,Rh} = 150$ Hz.

The same procedure using (+)-renorphos gave (+)-16 as ruby red crystals (72%). See Table I for selected physical data.

Preparation of 15 and 16 as Powders.¹⁶ (-)-norphos (500 mg, 1.08 mmol) and bis(norbornadiene)- μ,μ' -dichlorodirrhodium (260 mg, 0.58 mmol) were stirred in methanol (4 mL) under nitrogen for 1 h. Sodium perchlorate (390 mg, 3.2 mmol) in water (3 mL) was added portionwise over 2 h with vigorous stirring. After the addition was

complete, the reaction mixture was stirred for 1 h and then filtered and washed with water (2×10 mL) to give **15** as an orange-red powder (750 mg, 91%), mp 235 °C dec. The spectroscopic properties of this material were identical with those of **15** obtained as red crystals (above).

A similar procedure for (+)-renorphos gave (+)-**16** in 96% yield as an orange-red powder with spectroscopic properties identical with those of **16** obtained in crystalline form.

Catalytic Hydrogenations. Hydrogenations were performed on a standard hydrogenation manifold which allowed evacuation and pressurization with either hydrogen or inert gas. The hydrogen gas was passed through a long column of MnO on Vermiculite to remove any oxygen present. Crude kinetic measurements involved following the rate of dihydrogen uptake at ambient temperature (24 ± 1 °C) at 1.6 atm pressure. The following are typical procedures which employ cationic and in situ generated catalysts.

(a) **Hydrogenation of 4 with 15 as Catalyst Precursor.** The catalyst precursor (-)-**15** (7.1 mg, 9.4×10^{-3} mmol) was introduced into a three-necked 25-mL flask equipped with a magnetic stirrer. The flask was fitted onto a condenser attached to the hydrogenation line, and the second neck was sealed with a new septum. The system was evacuated and pressurized with 1 atm of H₂ three times, and then dry, degassed methanol (3 mL) was introduced by syringe through the septum. The resulting solution was stirred under 1 atm H₂ for 1 h, and then the substrate **4** (160 mg, 0.130 mmol) in degassed methanol (3 mL) was added by syringe to the yellow catalyst solution. The solution immediately turned red and hydrogen uptake commenced. The hydrogen pressure was maintained manually at 1.6 atm with the use of a leveling bulb and uptake of hydrogen was followed. Rate data are presented in Table II. The cessation of hydrogen uptake (40-min reaction time) was accompanied by the return to a yellow color of the reaction mixture. The resulting solution was stirred with Dowex-50W hydrogen resin (0.5 g) for 1 h, and the solvent was removed under vacuum to give (*S*)-**5** (158 mg, 97%), $[\alpha]_D^{25} 45.1^\circ$ (*c* 1.48, 95% EtOH).¹⁷

Similar experiments were carried out with (+)- or (-)-**16** and (diphos)Rh(NBD)ClO₄ on substrates **4**, **17**, and **19** and the results are summarized in Table II.

(b) **Hydrogenation of 4 with in Situ Generated Catalysts.** A degassed solution of (+)-**12** (4.4 mg, 9.5×10^{-3} mmol) and **13** (2.2 mg, 4.7×10^{-3} mmol) in dry degassed methanol (3 mL) were stirred in the above-described hydrogenation apparatus under an argon atmosphere for 0.5 h. The argon atmosphere was then replaced by hydrogen, and the resulting solution was stirred for 1 h. The substrate **4** (163 mg, 0.80 mmol) in degassed methanol (3 mL) was then introduced via syringe, and the rest of the procedure was as described above.

Similar procedures were carried out for (-)-**3** and diphos, and the results are reported in Table II.

Crystallographic Study of (+)-15. The preparation of (+)-**15** from (+)-**3** and **14** as described above gave tablet-shaped crystals, with faces of the forms (010), (011), and (110), elongated in the 100 direction. A crystal of appropriate size was mounted on a glass fiber and transferred to the Syntex P₂ autodiffractometer, where it was maintained at -100 °C in a stream of N₂ throughout all diffraction experiments. Details of characterization and of collection of intensity data are summarized in Table III. The measured intensities were reduced, corrected for absorption, and assigned standard deviations (with $p = 0.02$) as described elsewhere.²³

The structure was solved by the heavy-atom method and then refined by full-matrix least-squares methods, using the 3944 reflections with $I > 2.5\sigma_I$. The function minimized in refinement is $[\sum w(|F_o| - |F_c|)^2 / (m - s)]^{1/2}$, where the weight $w = \sigma(|F_o|)^{-2}$, the reciprocal square of the standard deviation of each observation, $|F_o|$. The conventional (R) and weighted (R_w) crystallographic agreement factors used to assess the structures are defined as $R = \sum ||F_o| - |F_c|| / \sum |F_o|$ and $R_w = [\sum w(|F_o| - |F_c|)^2 / \sum w|F_o|^2]^{1/2}$, respectively. Neutral atom scattering factors for Rh, Cl, P, C, O,²⁴ and H²⁵ were used in these calculations, and the real ($\Delta f'$) and imaginary ($\Delta f''$) corrections²⁴

Table VI. Bond Lengths, Angles, and Selected Torsion Angles^a for 15·C₄H₈O

(A) Bond Lengths (Å)			
Rh-P1	2.323 (2)	C3B-C4	1.324 (17)
Rh-P2	2.321 (2)	C4-C5	1.585 (10)
Rh-C12	2.183 (7)	C4-C7A	1.677 (17)
Rh-C13	2.195 (6)	C4-C7B	1.691 (17)
Rh-C15	2.214 (6)	C5-C6	1.549 (9)
Rh-C16	2.214 (7)	C11-C12	1.533 (9)
Rh-D12,13 ^b	2.081 (6)	C11-C16	1.546 (10)
Rh-D15,16 ^b	2.103 (6)	C11-C17	1.539 (10)
P1-PH1C1 ^c	1.823 (4)	C12-C13	1.359 (9)
P1-PH2C1	1.819 (4)	C13-C14	1.568 (9)
P1-C5	1.820 (6)	C14-C15	1.532 (9)
P2-PH3C1	1.827 (4)	C14-C17	1.543 (10)
P2-PH4C1	1.816 (4)	C15-C16	1.375 (10)
P2-C6	1.831 (6)	C1-O2	1.357 (9)
C1-C2A	1.412 (17)	C1-O3	1.394 (7)
C1-C2B	1.390 (19)	C1-O4	1.335 (10)
C1-C6	1.559 (10)	C1-O5	1.344 (15)
C1-C7A	1.690 (17)	O1-T2	1.450 (13)
C1-C7B	1.630 (17)	O1-T5	1.443 (12)
C2A-C3A	1.329 (21)	T2-T3	1.470 (17)
C2B-C3B	1.344 (22)	T3-T4	1.493 (22)
C3A-C4	1.324 (17)	T4-T5	1.415 (19)
(B) Bond Angles (Deg)			
P1-Rh-P2	86.4 (1)	C2B-C1-C7B	102.0 (9)
P1-Rh-D12,13	101.1 (2)	C6-C1-C7A	99.4 (7)
P1-Rh-D15,16	170.7 (2)	C6-C1-C7B	92.9 (7)
P2-Rh-D12,13	172.3 (2)	C1-C2A-C3A	110.3 (13)
P2-Rh-D15,16	103.3 (2)	C1-C2B-C3B	109.3 (15)
C12-Rh-C13	36.2 (2)	C2A-C3A-C4	110.2 (13)
C15-Rh-C16	36.2 (3)	C2B-C3B-C4	110.5 (13)
Rh-P1-PH1C1	119.0 (1)	C3A-C4-C5	118.8 (9)
Rh-P1-PH2C1	113.1 (1)	C3B-C4-C5	117.6 (9)
Rh-P1-C5	103.8 (2)	C3A-C4-C7A	102.5 (10)
PH1C1-P1-PH2C1	103.0 (2)	C3B-C4-C7B	101.5 (10)
PH1C1-P1-C5	108.6 (2)	C5-C4-C7A	93.2 (7)
PH2C1-P1-C5	109.2 (2)	C5-C4-C7B	99.0 (7)
Rh-P2-PH3C1	117.4 (1)	P1-C5-C4	131.6 (5)
Rh-P2-PH4C1	113.2 (1)	P1-C5-C6	106.7 (4)
Rh-P2-C6	103.3 (2)	C4-C5-C6	101.4 (5)
PH3C1-P2-PH4C1	108.2 (2)	P2-C6-C1	131.4 (5)
PH3C1-P2-C6	106.8 (2)	P2-C6-C5	106.5 (4)
PH4C1-P2-C6	107.4 (2)	C1-C6-C5	103.9 (5)
P1-PH1C1-PH1C2	117.7 (3)	C1-C7A-C4	84.8 (8)
P1-PH1C1-PH2C	122.2 (3)	C1-C7B-C4	86.2 (8)
P1-PH2C1-PH2C2	120.1 (3)	C12-C11-C16	102.7 (5)
P1-PH2C1-PH2C6	119.8 (3)	C12-C11-C17	100.5 (5)
P2-PH3C1-PH3C2	124.5 (3)	C16-C11-C17	98.1 (5)
P2-PH3C1-PH3C6	115.4 (3)	C11-C12-C13	107.3 (6)
P2-PH4C1-PH4C2	122.7 (3)	C12-C13-C14	106.7 (5)
P2-PH4C1-PH4C6	117.3 (2)	C13-C14-C15	102.7 (5)
C2A-C1-C6	108.6 (8)	C13-C14-C17	98.9 (5)
C2B-C1-C6	113.5 (9)	C15-C14-C17	99.4 (5)
C2A-C1-C7A	97.5 (9)	C14-C15-C16	106.4 (6)
C15-C16-C17	73.7 (5)	O4-C1-O5	104.2 (7)
C11-C17-C14	94.7 (5)	T2-O1-T5	107.8 (7)
O2-C1-O3	111.6 (5)	O1-T2-T3	106.7 (9)
O2-C1-O4	111.5 (6)	T2-T3-T4	108.4 (11)
O2-C1-O5	104.2 (7)	T3-T4-T5	105.6 (12)
O3-C1-O4	109.4 (6)	T4-T5-O1	111.2 (9)
(C) Selected Torsion Angles (Deg)			
Rh-P1-C5-C6	-47.4	D12,13-Rh-P1-C5	-162.0
Rh-P2-C6-C5	-48.5	D12,13-Rh-P2-C6	168.5
P1-Rh-P2-C6	15.4	D15,16-Rh-P1-C5	-167.1
P1-C5-C6-P2	63.6	D15,16-Rh-P2-C6	-164.4
P2-Rh-P1-C5	13.9		

^a Numbers in parentheses are estimated standard deviations in the units of the last significant digit for the parameter. ^b D12,13 and D15,16 represent the midpoints of the C12-C13 and C15-C16 double bonds, respectively. The coordinates of D12,13 are 0.75348, 0.85325, 0.68891 and of D15,16 are 0.79080, 0.95031, 0.79763. ^c An atom designated by PHxCy is carbon atom y on phenyl ring x.

(23) Riley, P. E.; Davis, R. E. *Acta Crystallogr., Sect. B* 1976, B32, 381. A listing of principal computer programs used in the crystallographic work also appears in this paper.

(24) "International Tables for X-ray Crystallography"; Kynoch Press: Birmingham, England, 1974; Vol. IV.

(25) Stewart, R. F.; Davidson, E. R.; Simpson, W. T. *J. Chem. Phys.* 1965, 42, 3175.

for anomalous dispersion were applied to the Rh, Cl, and P scattering curves.

Throughout the refinement, the phenyl rings were treated as rigid groups constrained with C-C = 1.392 Å, C-H = 1.00 Å, and all bond angles 120°, and with isotropic temperature factors for C varied individually while those for H were held fixed at 3.5 Å². Isotropic refinement omitting all nongroup H atoms approached convergence at $R = 0.080$ and $R_w = 0.088$. Anisotropic refinement was begun at this stage for all nongroup atoms, except the THF atoms which were always treated isotropically. When values of $R = 0.066$ and $R_w = 0.071$ were reached in the anisotropic refinement, unduly high thermal parameters for some of the carbons of the norphos ligand suggested the presence of disorder in this ligand. A difference density map, omitting the three carbons of the 1,2-ethylidene bridge and the methylene bridge of the norbornene ring system, revealed that these three carbons were each occupying two positions, related by a pseudo-two-fold axis approximately bisecting the P-Rh-P angle and approximately normal to the C5-C6 bond. Each of these six positions was described as being occupied by a half-weighted carbon atom, and these were treated isotropically in all subsequent refinement.²⁶

So that the assignment of absolute configuration could be tested, the structure was at this point subjected to two parallel refinements, one for each of the possible enantiomers. With the use of coordinates describing the *S,S* structure, convergence was achieved at $R = 0.052$ and $R_w = 0.056$, while the *R,R* structure could be refined only to $R = 0.054$ and $R_w = 0.059$. A statistical interpretation of the *R* factor ratio using Hamilton's test²⁷ indicated that the *R,R* configuration for (+)-**15** could be rejected in favor of *S,S* at a confidence level far exceeding 99.5%. This result is consistent with the assignment by Brunner.⁵

At this stage, a difference density map contained peaks at all computed hydrogen positions,²⁸ including those of the disordered

carbons. Hydrogens were included at these idealized positions and assigned isotropic temperature factors corresponding to the thermal motion of the carbons to which they were attached. Attempts to refine these hydrogen temperature factors resulted in unreasonable values, so these were held fixed at their initial values while positions were allowed to vary. Hydrogens on the THF molecule were also held fixed in their initial idealized positions. Final convergence of the refinement was obtained with $R = 0.047$ and $R_w = 0.048$. Inclusion of all reflections in a final structure factor calculation gave $R = 0.062$ and $R_w = 0.048$. A final difference density map contained only small peaks ($<0.9 \text{ e } \text{Å}^{-3}$).

Final fractional crystallographic coordinates and anisotropic temperature factors for the nonhydrogen, nongroup atoms appear in Table IV. Rigid group parameters used to describe the phenyl rings are presented in Table V. Bond lengths, angles, and selected dihedral angles are contained in Table VI.

Observed and calculated structure factor amplitudes, final parameters for nongroup hydrogen atoms, and fractional crystallographic coordinates and temperature factors for the rigid group atoms and for the atoms in THF appear in supplementary tables.²⁶

Acknowledgment. Financial support by the Air Force Office of Scientific Research (to E.P.K., Grant AFOSR-79-0090) and the Robert A. Welch Foundation (to E.P.K., Grant F-573, and R.E.D., Grant F-233) is gratefully acknowledged. We are indebted to the National Science Foundation for the purchase of a Syntex P2 diffractometer (Grant GP-37028).

Registry No. (-)-**2**, 71075-23-5; (-)-**3**, 71042-54-1; **4**, 55065-02-6; (-)-**11**, 78822-58-9; (-)-**12**, 78803-92-6; **13**, 12257-42-0; **14**, 32354-50-6; (-)-**15**-C₄H₈O, 78791-09-0; (+)-**16**, 78803-86-8; **17**, 5429-56-1; **19**, 97-65-4; **21**, 32799-34-1; (+)-**12**, 78803-93-7.

Supplementary Material Available: Tables of observed and calculated structure factor amplitudes (Supplementary Table I), anisotropic thermal parameters (Supplementary Table II), derived fractional coordinates for rigid atom groups (Supplementary Table III), and fractional coordinates and isotropic thermal factors for atoms in the tetrahydrofuran molecule (Supplementary Table IV) (26 pages). Ordering information is given on any current masthead page.

(26) Evrard, G.; Thomas, R.; Davis, B. R.; Bernal, I. J. *Organomet. Chem.* **1977**, *124*, 59-70.

(27) Hamilton, W. C. *Acta Crystallogr.* **1965**, *18*, 502.

(28) Idealized hydrogen positions were generated by the use of the local program HIDEAL written by R. C. Collins.

Contribution from the General Education Department, Kogakuin University, Hachioji-shi, Tokyo 193, Japan

Preparation and Characterization of Some Chromium(III) Complexes of the Forms [Cr(L- or D-asp)(L-his)] and [Cr(L-asp)₂]⁻ (asp = Aspartate and his = Histidinate Ions)

MASATOSHI WATABE,* HISAO YANO, YOSHIO ODAKA, and HARUMI KOBAYASHI

Received November 13, 1980

Mixed-ligand chromium(III) complexes of the form [Cr(L- or D-asp)(L-his)] and [Cr(L-asp)₂]⁻ were prepared. Isolated isomers of each complex were assigned structures on the basis of their visible spectra and high-speed chromatograms. The CD spectra of the [Cr(L- or D-asp)(L-his)] complexes are similar to those of the [Co(L- or D-asp)(L-his)] complexes, permitting tentative structural assignments for three isomers of the [Cr(L-asp)₂]⁻ complexes. The observed distribution of the isomers suggests that in these complexes, as well as in previously reported [Co(L- or D-asp)(L-his)] complexes, amino groups avoid being trans to each other.

Introduction

Only a few Cr(III) complexes containing bis(tridentate) amino acidate ligands have been prepared.¹⁻³ Though three geometrical isomers (*fac-cis*(N), *fac-trans*(N), and *mer-trans*(N)) are possible for the Cr^{III}N₂O₄ complexes coordinating bis(iminodiacetate) or bis((methylimino)diacetate) ligands, only one each has been prepared for the former complex, which exists as the *cis*(N) isomer, and for the latter

complex, being *trans*(N). While three isomers have been prepared for the [Cr(L-asp)₂]⁻ complexes, their geometrical configurations have not been assigned even tentatively because their UV and CD spectra resemble each other.³

We have reported so far preparations of the [Co(A)(B)] type complexes that take the form of Co^{III}N₃O₃, where A = L- or D-aspartate or iminodiacetate and B = L-histidinate, L-2,4-diaminobutyrate, or L-ornithinate.⁴⁻¹¹ Though every

(1) A. Uehara, E. Kyuno, and R. Tsuchiya, *Bull. Chem. Soc. Jpn.*, **43**, 1394 (1970).

(2) J. A. Weyh and R. E. Hamm, *Inorg. Chem.*, **7**, 2431 (1968).

(3) G. Grouhi-Witte and E. Weiss, *Z. Naturforsch., B: Anorg. Chem., Org. Chem.* **31B**, 1190 (1976).

(4) M. Watabe, K. Onuki, and S. Yoshikawa, *Bull. Chem. Soc. Jpn.*, **48**, 687 (1975).

(5) M. Watabe and S. Yoshikawa, *Bull. Chem. Soc. Jpn.*, **48**, 2185 (1975).

(6) M. Watabe, S. Kawai, and S. Yoshikawa, *Bull. Chem. Soc. Jpn.*, **49**, 1848 (1976).